CHANNEL MODELS FOR COOPERATIVE MIMO SYSTEMS

A DISSERTATION

Submitted in partial fulfillment of the
requirements for the award of the degree
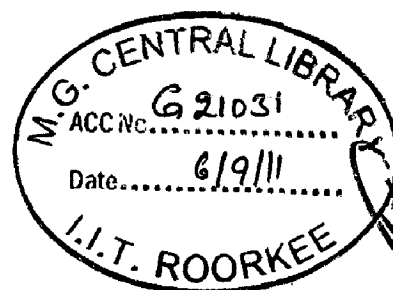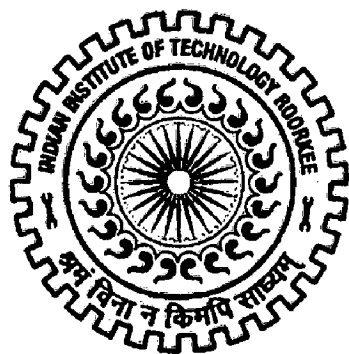of
MASTER OF TECHNOLOGY
in
ELECTRONICS AND COMMUNICATION ENGINEERING
(With Specialization in Communication Systems)

By

SUMEER LAMBA

DEPARTMENT OF ELECTRONICS AND COMPUTER ENGINEERING
INDIAN INSTITUTE OF TECHNOLOGY ROORKEE
ROORKEE -247 667 (INDIA)
JUNE, 2011

CANDIDATE'S DECLARATION

I hereby declare that the work, which is presented in this dissertation report entitled, "**Channel Models for Cooperative MIMO Systems**" towards the partial fulfillment of the requirements for the award of degree of **MASTER OF TECHNOLOGY** with specialization in Communication Systems, submitted in the Department of Electronics and Computer Engineering, Indian Institute of Technology, Roorkee (India) is an authentic record of my own work carried out during the period from May 2010 to June 2011, under the supervision of **Dr. D. K. Mehra, Professor, Department of Electronics and Computer Engineering, Indian Institute of Technology, Roorkee.**

I have not submitted the matter embodied in this dissertation for the award of any other Degree or Diploma.

Date: 28 June 2011
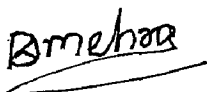
Place: Roorkee

SUMEER LAMBA

CERTIFICATE

This is to certify that the above statement made by the candidate is correct to the best of my knowledge and belief.

Date: 28.06.2011

Place: Roorkee

Dr. D.K. MEHRA
Professor
E&C Department
IIT Roorkee
Roorkee-247667(India)

i

Acknowledgements

First and foremost, I would like to express my profound sense of respect and gratitude to my guide, Dr. D. K. Mehra for his invaluable guidance and constant encouragement throughout the dissertation. He provided me valuable support, right from introducing me to the topic to writing this thesis. I consider myself fortunate to have my dissertation done under him.

I would like to thank my classmates for sharing their knowledge and constant support during the course of dissertation work. Thanks are due to the staff of Signal Processing Lab, Department of Electronics and Computer Engineering, IIT Roorkee, Roorkee for providing necessary facilities.

I wish to pay my humble tribute to my mother who encouraged me to pursue this M Tech program. I am grateful to my wife and children who provided me the moral support and positive environment to accomplish this goal.

Finally, I would like to extend my thanks to all those who have directly or indirectly contributed towards this work.

SUMEER LAMBA

Abstract

Cooperative MIMO is a promising technology which can exploit the spatial diversity gains inherent in multiuser wireless systems without the need of multiple antennas at each node. Cooperative MIMO technology finds its application in cellular systems as well as resource constrained wireless sensor network in which the nodes can cooperate to optimally allocate resources, so as to maximize the performance and network lifetime.

A deep understanding of the channel is necessary before setting up any wireless network. The various cooperative relaying protocols like Amplify and Forward, Detect and Forward and Coded Cooperation are briefly explained in this thesis. The statistical properties like time domain correlation, doppler spectrum, level crossing rate and signal to noise ratio of the fixed gain relay channel are elaborated which provides understanding about the characteristics of the relay fading channel. The tapped delay model forms a basis for simulation of such fading channels. A tapped delay model for a MIMO channel is presented before giving an overview of standardized point to point MIMO channel models like WINNER II model, 3GPP SCM, SUI and 802.16j channel model. While many issues in cooperative MIMO channel modeling have been covered by the existing standardized point-to-point MIMO channel models, there are still some challenges that remain to be addressed, which are concisely brought out.

The mobile to mobile (M2M) channel is an integral part of Cooperative MIMO systems. The "double-ring" scattering model proposed by Patel et. al. is used to simulate the M2M channels. This double ring model is verified in terms of statistical properties like pdf of complex envelope, autocorrelation, variance of the autocorrelation and level crossing rate (LCR). The performance of DPSK in terms of BER and outage probability over such M2M channel is evaluated and compared with the available analytical results. The single relay acting as Amplify and Forward (A&F) node forms the simplest scenario for cooperative communication. The concept of double ring model is extended to simulate this relay channel as three ring model, in which the ring of scatterers is also considered around the relay node. Under flat fading conditions, the overall channel from the source to the destination via the relay in A&F systems is "double Rayleigh" with properties quite different from a typical cellular channel. The three ring model is verified in terms of statistical properties such as the envelope pdf, autocorrelation, level crossing rate and doppler spectrum. The performance of

DPSK over such a relay channel is evaluated. The plots of BER versus SNR are obtained and compared with the analytic results.

The Maximum Ratio Combining (MRC) is considered to study the multichannel cooperative diversity (CD) networks. The double ring and three ring model are used to simulate these CD networks. The performance of BPSK over these multichannel networks is obtained in terms of BER which validate the diversity gains associated with cooperation. The doppler is introduced in the channel model to see the effect of mobility of terminals on channel coefficients.

Contents

List of Figures

Chapter-1

Introduction

Multiple-input multiple-output (MIMO) is an advanced technology that can effectively exploit the spatial domain of mobile fading channels to bring significant performance improvements to wireless communication systems. The point-to-point conventional MIMO system (Fig. 1.1) requires both the transmitter and receiver of a communication link to be equipped with multiple antennas. The wireless devices like mobile phones are not able to support multiple antennas due to size, cost and hardware limitations. The concept of Cooperative MIMO utilizes distributed antennas on multiple radio devices to achieve some benefits similar to those provided by conventional MIMO systems. This helps to achieve the higher data rates of the order of 50 b/s/Hz which cannot be achieved with SISO systems within the constraints of bandwidth and power, as illustrated by Dr. Paulraj et. al. in [1]. The performance improvements resulting from such systems are due to array gain, diversity gain, spatial multiplexing gain and interference reduction. Since the Cooperative MIMO utilizes distributed antennas on multiple radio devices, it is also known as distributed or virtual MIMO.
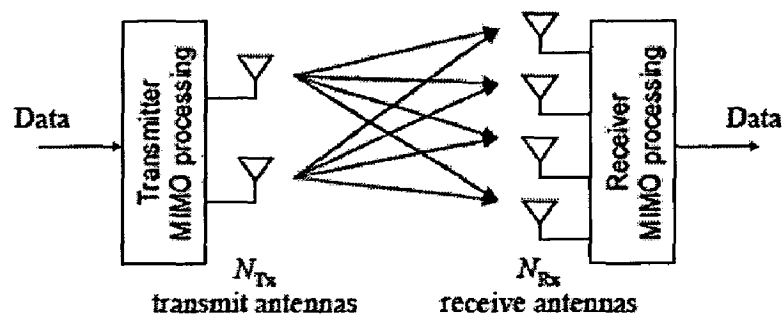
Figure 1.1 MIMO system representation

The basic idea of cooperative MIMO is to group multiple devices into virtual antenna arrays (VAAs) to emulate MIMO communication. Cooperative techniques can be developed for both ad-hoc networks as well as cellular networks. The mobile or fixed nodes act alternatively as a source (S), a relay (R) or a destination (D). These advantages of Cooperative MIMO makes it most eligible technology for forthcoming 4G systems which can

cooperation, the base station receives two independently faded versions of the signal and can make better decisions on the detection of information. It has been shown that for the two-user case, this method achieves diversity order of two, which is the best possible outcome at high SNR. In A & F strategy, it is assumed that the base station knows the inter-user channel coefficients to do optimal decoding. Therefore, some mechanism of exchanging or estimating this information is incorporated.

Detect and Forward Method

This method is perhaps closest to the idea of a traditional relay. In this method, a user attempts to detect the partner's bits and then retransmits the detected bits. The partners may be assigned mutually by the base station, or via some other technique. An example of decode-and-forward signaling can be found in the work of Sendonaris, Erkip and Aazhang [2] which has inspired much of the recent activity in this area. This work presents analysis and a simple code-division multiple access (CDMA) implementation of decode-and-forward cooperative signaling. In this scheme, two users are paired to cooperate with each other. Each user has its own spreading code denoted by $c_1(t)$ and $c_2(t)$. The two user's data bits are denoted as $b_i^{(n)}$ Where $i = 1, 2$ are the user indices and n denotes the time index of information bits. Factors $a_{i,j}$ denote signal amplitudes, and hence represent power allocation to various parts of the signaling. The term $\hat{b}_i^{(n)}$ denotes the user's estimate of ith partner's bit. Each signaling period consists of three bit intervals.

Consider $X_1(t)$ be the signal of user 1 and $X_2(t)$ be the signal of user 2.

I^{st} Interval	IInd Interval	IIIrd Interval
$X_1(t) = a_{11}b_1^{(1)}c_1(t)$,	$a_{12}b_1^{(2)}c_1(t)$,	$a_{13}b_1^{(2)}c_1(t) + a_{14}\hat{b}_2^{(2)}c_2(t)$
$X_2(t) = a_{21}b_2^{(1)}c_2(t)$,	$a_{22}b_2^{(2)}c_2(t)$,	$a_{23}\hat{b}_1^{(2)}c_1(t) + a_{24}b_2^{(2)}c_2(t)$

Explanation - In the first and second intervals, each user transmits its own bits. Each user then detects the other user's second bit. In the third interval, both users transmit a linear combination of their own second bit and the partner's second bit, each multiplied by the appropriate spreading code. The transmit powers for the first, second, and third intervals are variable, and by optimising the relative transmit powers according to the conditions of the uplink and inter user channels, this method provides adaptability to channel conditions. The

3

To avoid the problem of error propagation, Laneman [5] proposed a selective decode-and-forward method where, at times when the fading channel has high instantaneous signal-to noise ratio (SNR), users detect and forward their partner's data, but when the channel has low SNR, users revert to a non-cooperative mode. This is not like the adaptability of coefficients $a_{i,j}$ provided by the method of Sendonaris, and has shown to perform quiet well.

Coded Cooperation

Coded cooperation is a method that integrates cooperation with channel coding. The advantages of coded cooperation under different scenarios were illustrated by Hunter and Nostratinia in [6,7]. Coded cooperation works by sending different portions of each user's code word via two independent fading paths. The basic idea is that each user tries to transmit incremental redundancy to its partner. Whenever that is not possible due to channel between two users going into deep fade, they automatically revert to a non-cooperative mode. The key to the efficiency of coded cooperation is that all this is managed automatically through code design, with no feedback between the users. The users divide their source data into blocks that are augmented with cyclic redundancy check (CRC) code. In coded cooperation, each of the users' data is encoded into a code word that is partitioned into two segments, containing N_1 bits and N_2 bits, respectively. This concept can be better explained with the following example. Consider that the original codeword has $N_1 + N_2$ bits. Puncturing this codeword down to N_1 bits, we obtain the first partition, which itself is a valid (weaker) codeword. The remaining N_2 bits are the puncture bits. Likewise, the data transmission period for each user is divided into two time segments of N_1 and N_2 bit intervals, respectively. These time intervals may be called as frames.

Frame 1- For the first frame, each user transmits a code word consisting of the N_1-bit code partition.

Frame 2- Each user also attempts to decode the transmission of its partner. If this attempt is successful (determined by checking the CRC code) in the second frame the user calculates and transmits the second code partition of its partner containing N_2 code bits. Otherwise, the user transmits its own second partition, again containing N_2 bits

Thus, each user always transmits a total of $N = N_1 + N_2$ bits per source block over the two frames. We define the level of cooperation as N_2/N, the percentage of the total bits for each

fixed (BS) to mobile (MS) channel. The mobility of both the transmitter (Tx) and the receiver (Rx) results in different statistical properties of mobile-to-mobile wireless channels, as described first by Akki and Haber [11,12] for non-line of sight (N-LOS) scenario. A model based on approximating the continuous Doppler spectrum by a discrete line spectrum was presented by Wang and Cox to simulate mobile-to-mobile channels in [13] but this channel model has several drawbacks like cross correlation between I and Q components is not zero and existence of periodicity in the autocorrelation of the complex envelope. The Sum-of-sinusoids (SoS) model for cellular channels was presented by Zheng and Xiao in [14, 15]. The same SoS approach was used by Patel et. al. in [16] who proposed a statistical "double-ring" scattering model to simulate the mobile-to-mobile channels. They also illustrated temporal statistical properties such as the auto-correlation, level crossing rate (LCR) etc. of relay channel consisting of the BS (fixed), the relay (mobile) and the MS (mobile) in [17]. The performance analysis in terms of BER of multiple branches cooperative network is given in [18] which is based on specific assumptions like high SNR between the links.

1.3   Applications of Cooperative MIMO

Cooperative MIMO in Cellular Systems [19]

Coordinated Multipoint Transmission-   CoMP is promising technique to combat inter-cell interference and improve cell edge performance which is difficult to be achieved with the conventional cellular communication. The system configuration is illustrated in Fig 1.4(a). The idea is to share data and channel state information (CSI) among neighboring base stations (BSs) to coordinate their transmissions in the downlink and jointly process the received signals in the uplink. CoMP techniques can effectively turn otherwise harmful inter-cell interference into useful signals, allowing significant power gain, channel rank advantage, and diversity gain. The promised advantages of CoMP rely on a high-speed backbone enabling the exchange of information (e.g., data, control information, and CSI) between the BSs. CoMP has been studied intensively in both academia and industry over recent years, and is a very strong candidate technology for 4G standards. CoMP systems are concerned with the BS to MS channels, which are fixed-to-mobile channels.

Fixed Relays-   The fixed relays are low-cost and fixed radio infrastructures without wired backhaul connections. They store data received from the BS and forward to the MSs, and

shown in Fig 1.4(b), fixed relay systems involve different types of links, including BS-MS, BS-RS, RS-RS, and RS-MS links. The BS-RS and RS-RS channels are fixed to fixed channels while the BS-MS and RS-MS channels are fixed to mobile channels.

Mobile Relays-   As the name suggests, the RSs in the Mobile relay configuration are mobile and they are not deployed as the infrastructure of a network as in a fixed relay setup. Mobile relays are therefore more flexible in accommodating varying traffic patterns and adapting to different propagation environments. For example, when a target MS temporarily suffers from bad channel conditions or requires relatively high-rate service, its neighboring MSs can help to provide multihop coverage or increase the data rate by relaying information to the target MS. Moreover, mobile relays enable faster and lower-cost network rollout. Similar to fixed relays, mobile relays can enlarge the coverage area, reduce the overall transmit power, and increase the capacity at cell edges. On the other hand, due to their opportunistic nature, mobile relays are less reliable than fixed relays since the network topology is highly dynamic and unstable. As shown in Fig 1.4(c), two types of mobile relay systems can be distinguished: moving networks and mobile user relays. The moving network employs dedicated RSs on moving vehicles (e.g., trains) to receive data from the BS and forward to the user MSs onboard, and vice versa. The purpose of the moving network is to improve coverage on the vehicle. The mobile user relay enables distributed MSs to self-organize into a wireless ad hoc network, which complements the cellular network infrastructure using multihop transmissions. Theoretical studies have shown that mobile user relays have a fundamental advantage in that the total network capacity, measured as the sum of the throughputs of the users, can scale linearly with the number of users given sufficient infrastructure supports. Mobile user relays are therefore a desirable enhancement to future cellular systems. However, mobile user relays also face huge challenges in routing, radio resource management, and interference management. The major disadvantage of, mobile user relays is that MS batteries can be used up by relay transmissions even if the user does not use them. Mobile user relays also complicate the billing problem (i.e., who shall pay the bill when a user helps other users as a relay). Currently, moving networks are supported by the IEEE 802.16j WiMAX standard. A number of advanced mobile relays concepts are being evaluated for the 4G standard. Moving networks involve the BS-MS, BS-RS, and RS-MS links, where the BS-MS and BS-RS channels are F2M channels, while the RS-MS channels are F2F or F2M channels. Mobile user relays involve BS-MS and MS-MS links, where the BS-MS channels are F2M channels, while the MS-MS channels are M2M channels.

Chapter-2

Cooperative MIMO Channel Model

The MIMO technology has made its way from pure theoretical analysis that promised enormous capacity gains to actual products for the wireless market. There are numerous MIMO techniques which have not been sufficiently tested under realistic propagation conditions and hence their integration into real applications can still be considered in its infancy. Moreover, the physical testing of the technology under realistic propagation conditions is highly expensive and cumbersome. This fact underlines the importance of physically meaningful, yet easy to use methods to understand and mimic the wireless channel. There are existing standardized MIMO channel models, such as the 3GPP spatial channel model (SCM) [21], the WINNER II channel model [22] and the Stanford University Interim (SUI) channel model [23] which can be used to simulate individual point-to-point channels.

Since the Cooperative MIMO utilizes distributed antennas on multiple radio devices, it involves multiple point-to-point links. Its channel model should consider not only the properties of the individual links, but also the system-level variations (or heterogeneity) and correlation of multiple links in a multi-cell environment. Also, for cooperative MIMO using mobile relays, realistic mobile-to-mobile (M2M) channel models are required for channels between mobile users. The realistic cooperative MIMO channel models are indispensable to accurately evaluate and compare the performance of different transmission technologies for cooperative MIMO cellular systems. The standardized cooperative MIMO channel model is not yet available. The existing point-to-point MIMO channel models can be applied only to a certain extent to model cooperative MIMO channels [19]. Many new challenges remain in cooperative MIMO channel modeling, such as how to model mobile-to-mobile channels, and how to characterize the heterogeneity and correlation of multiple links at the system level appropriately.

multipath component. Therefore, this tapped delay line model will have as many taps as the number of multipath components having discernable amplitude levels. Such tapped delay line model is shown in figure 2.1.
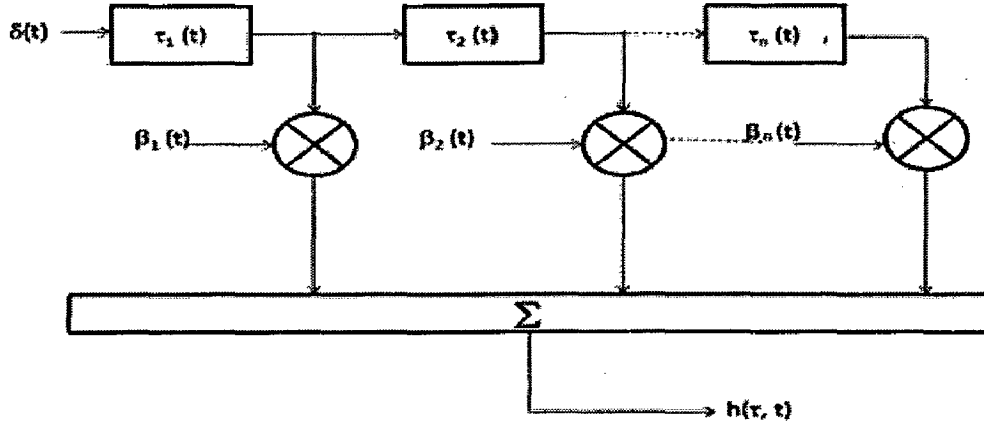
$$\beta_n(t) = \alpha_n(t)e^{-j2\pi f_c \tau_n(t)}$$

Fig. 2.1 Tapped Delay Line Model

Now, Consider a MIMO system with N_T number of transmit antennas and N_R receive antennas [23]. If $h_{i,j}(\tau, t)$ is the impulse response between the j^{th}($j=1,2\ldots\ldots N_T$) transmit antenna and the i^{th}($i=1,2\ldots\ldots N_R$) receive antenna, the MIMO channel can be represented by $N_R \times N_T$ matrix $H(\tau, t)$ which can be written as

$$H(\tau, t) = \begin{bmatrix} h_{1,1}(\tau, t) & h_{1,2}(\tau, t) \cdots & h_{1,N_T}(\tau, t) \\ h_{2,1}(\tau, t) & h_{2,2}(\tau, t) \cdots & h_{2,N_T}(\tau, t) \\ \vdots & \vdots & \ddots & \vdots \\ h_{N_R,1}(\tau, t) & h_{N_R,2}(\tau, t) & h_{N_R,N_T}(\tau, t) \end{bmatrix} \qquad (2.5)$$

If the signal $s_j(t)$ is launched from the jth transmit antenna, the signal received at the ith receive antenna is given by

$$y_i(t) = \sum_{j=1}^{N_T}[h_{i,j}(\tau, t) * s_j(t)], \quad i = 1,2\ldots\ldots\ldots N_R$$

In matrix notation, the input output relation for the MIMO channel may be expressed as

$$Y(t) = H(\tau, t) \times S(t) \qquad (2.6)$$

13

2. The WINNER II model uses the same modeling approach for both indoor and outdoor environment, outdoor-to-indoor and indoor-to-outdoor scenarios, elevation in indoor scenarios and scenario-dependent polarisation modeling.

3. WINNER II channel models can be used in link level and system level performance evaluation of wireless systems, as well as comparison of different algorithms, technologies and products. These models can be applied not only to WINNER II system, but also any other wireless system operating in $2 - 6$ GHz frequency range with maximum 100 MHz RF bandwidth.

4. The models are scalable from a single single-input-single-output (SISO) or multiple-input-multiple-output (MIMO) link to a multi-link MIMO scenario including polarisation among other radio channel dimensions.

5. The models supports multi-antenna technologies, polarisation, multi-user, multi-cell, and multi-hop networks.

6. Intracluster delay spread is introduced in the WINNER II channel model to account for better delay resolution and consequently broader bandwidths.

Modeled parameters [22]

Parameters used in the WINNER II Channel Models can be divided into large scale parameters (LSP) and Support parameters which are listed below.

<u>Large Scale Parameters</u>
- Delay spread and distribution
- Angle of Departure spread and distribution
- Angle of Arrival Spread and distribution
- Shadow Fading standard deviation
- Ricean K-factor

<u>Support Parameters</u>
- Scaling parameter for Delay distribution
- Cross-polarisation power ratios
- Number of clusters
- Cluster Angle Spread of Departure
- Cluster Angle Spread of Arrival
- Per Cluster Shadowing

The mean and standard deviation of the pdfs of these parameters are specified for each scenario in WINNER II generic model, as shown in table 2.1. These statistics of various parameters are used while simulating a channel model for a particular scenario.

Table 2.1 Table of Parameters for WINNER II Generic Model

SCENARIO		AI		A2/B4/C4	B1		B3		C1		C2		D1	
PARAMTERS		LOS	NLOS	NLOS	LOS	NLOS	LOS	NLOS	LOS	NLOS	LOS	NLOS	LOS	NLOS
Delay Spread (DS) $\log_{10}(s)$	μ	-7.42	-7.60	-7.39	-7.44	-7.12	7.53	7.41	7.23	7.12	7.39	6.63	-7.80	7.60
	σ	.27	.19	.36	.25	.12	.12	.13	.49	.33	.63	.32	.57	.48
AoD Spread (ASD) $\log_{10}[°]$	μ	1.64	1.73	1.76	.40	1.19	1.22	1.05	.78	.90	1	.93	.78	.96
	σ	.31	.23	.16	.37	.21	.18	.22	.12	.36	.25	.22	.21	.45
AoA Spread (ASA) $\log_{10}[°]$	μ	1.65	1.69	1.25	1.40	1.55	1.58	1.7	1.48	1.65	1.7	1.72	1.20	1.52
	σ	.26	.14	.42	.20	.20	.23	.1	.20	.30	.19	.14	.18	.27
Shadow Fading (SF) dB	σ	3	4	7	3	4	3	4	4/6*	8	4/6*	3	4/6*	8
Delay Distribution		Exp	Exp	Exp	Exp	Uniform <800 ns	Exp	Exp	Exp	Exp	Exp	Exp	Exp	Exp
K-Factor	μ	7	N/A	N/A	9	N/A	2	N/A	9	N/A	7	N/A	7	N/A
	σ	6	N/A	N/A	6	N/A	3	N/A	7	N/A	3	N/A	6	N/A
No of Clusters		12	16	12	8	16	10	15	15	14	8	20	11	10
No of Rays/ Cluster		20	20	20	20	20	20	20	20	20	20	20	20	20

2.3   3GPP Spatial Channel Model

The spatial channel model (SCM) [21,25,27] is a geometry-based stochastic model, developed by 3GPP which is used as a common reference for evaluating different MIMO concepts in outdoor environment at a center frequency of 2 GHz and a system bandwidth of 5 MHz. The SCM was dedicated to outdoor propagation and defined three main propagation scenarios: suburban macrocell, urban macrocell, and urban microcell. LOS condition is defined for the urban microcell scenario only and not for the suburban or urban macrocell cases due to low probabilities of LOS occurrence. The SCM consists of two parts:-

(i) Calibration model, and

(ii) System-simulation model.

Calibration Model

The calibration model is an over-simplified channel model whose purpose is to check the correctness of simulation implementations. The calibration model is not intended for performance assessment of algorithms or systems. The calibration model, as described in the 3GPP/3GPP2standard, can be implemented either as a physical model or as an analytical model. The physical model is a non-geometrical stochastic physical model. It describes the wideband characteristics of the channel as a tapped delay line. Taps with different delays are independently fading and each tap is characterized by its own power azimuth spectrum (which is uniform or Laplacian), angular spread (ΔS), and mean direction, at both the MS and the BS. Since the parameters like angular spread, mean direction etc. are fixed, the model represents stationary channel conditions. The Doppler spectrum is defined implicitly by introducing speed and direction of travel of the MS. The model also defines a number of antenna configurations.

Simulation Model

The SCM intended for performance evaluation is called the simulation model. The model is a physical model and distinguishes between three different environments: urban macrocell, suburban macrocell, and urban microcell. The model structure and simulation methodology are identical for all these environments, but the parameters like angular spread, delay spread

geometries, and orientations can be chosen arbitrary which makes the model antenna independent. When all the parameters and antenna effects are defined, analytical formulations can be extracted from the physical model. Each drop results in a different correlation matrix for the analytical model. In addition to the characteristics described above, the simulation model has several optional features which are listed below.

(i)   Polarization model

(ii)   Far scatterer cluster model which is limited to use with the urban macro-cell where the first cluster will be the primary cluster and the second will be the far scattering cluster.

(iii)   One LoS component for the microcellular case

(iv)   Modified distribution of the angular distribution at the MS, which emulates propagation in an urban street canyon.

2.4   Stanford University Interim (SUI) and IEEE 802.16j Channel Models

The Stanford university interim (SUI) channel model is a set of 6 channel models representing three types of terrain and a variety of Doppler spreads, delay spread and LOS/N-LOS site conditions. The three types of terrains covered by these models are A, B and C. Type A is associated with maximum path loss and is appropriate for hilly terrain with moderate to heavy foliage densities. Type C is associated with minimum path loss and applies to flat terrain with light tree densities. Type B is characterised with either flat terrains with moderate to heavy tree densities or hilly terrains with light tree densities. SUI models have been specifically designed for a cell size of 7 km, receiver antenna height of 6 m, base station antenna height of 30 m and beamwidth of 120° [23]. They were developed for macrocellular fixed wireless access networks operating at 2.5 GHz and were further enhanced in the framework of the IEEE 802.16a standard.

The general structure for the SUI channel model is shown in figure 2.3. This structure is for Multiple Input Multiple Output (MIMO) channels and includes other configurations like Single Input Single Output (SISO) and Single Input Multiple Output (SIMO) as subsets. The SUI channel structure is the same for the primary and interfering signals. The input mixing matrix models the correlation between input signals, if multiple transmitting antennas

$$H(\tau, t) = \begin{bmatrix} e^{j\Phi_1} & 0 \\ 0 & e^{j\Phi_2} \end{bmatrix} \begin{bmatrix} 1 & \rho_r \\ \rho_r & 1 \end{bmatrix} \begin{bmatrix} h_{11}(\tau, t) & 0 \\ 0 & h_{22}(\tau, t) \end{bmatrix} \begin{bmatrix} 1 & \rho_t \\ \rho_t & 1 \end{bmatrix} \begin{bmatrix} e^{j\Phi_3} & 0 \\ 0 & e^{j\Phi_4} \end{bmatrix} \quad (2.7)$$

$$h_{11}(\tau, t) = h_{11}(0, t)\,\delta(\tau) + \sum_{i=1,2} h_{11}(i, t)\,\delta(\tau - \tau_i) \qquad (2.8)$$

$$h_{22}(\tau, t) = h_{22}(0, t)\,\delta(\tau) + \sum_{i=1,2} h_{22}(i, t)\,\delta(\tau - \tau_i) \qquad (2.9)$$

where $h_{11}(i, t)$ and $h_{22}(i, t)$ ($i=0,1,2$) are the tapped delay line weights, which are independent complex Gaussian random variables with a K-Factor (K_i) and delay (τ_i). ρ_r and ρ_t are the correlation parameters that can be used to adjust the degree of fading signal correlation. Each tap of any SUI channel is characterized by a single antenna correlation coefficient at the user's terminal (UT), irrespective of the UT array configuration, while the antenna correlation at the base station (BS) is taken as equal to zero, assuming a large BS antenna spacing [25]. All of these parameters are specified for each of the six SUI models. The phases Φ_i ($i=1,2,3,4$) can be chosen arbitrarily to reflect the antenna array geometry and AOD/ AOA. Using the general structure of the SUI Channel and assuming the appropriate scenario, SUI channel can be constructed which is the representation of the real propagation channel.

IEEE 802.16j Channel Model [19,28]

The IEEE 802.16j channel model is based on the Stanford university interim (SUI) model and it was extended in 2007 to cover relay scenarios in IEEE 802.16j WiMAX systems. It supports a center frequency of 5 GHz and a maximum system bandwidth of 20 MHz. The IEEE 802.16j channel model is a correlation-based stochastic models (CBSM) having fixed number of delay line taps as three. Each tap represents a resolvable path or a cluster of scatterers with a different delay. CBSMs assume Rayleigh or Ricean fading for each tap, and then carefully introduce autocorrelation and cross-correlation into the MIMO channel matrix via Doppler filtering and spatial filtering. CBSMs are relatively simple and computationally efficient. They also explicitly address the correlation properties of MIMO channel matrices, providing a useful reference for system designers. The drawback of CBSMs comes from the over simplification and consequently an unrealistic representation of link variations in system- level simulations.

IEEE 802.16j presents nine types of channel models. Types A–H and Type J. These scenarios are commonly experienced in WiMAX multi-hop relay networks. Similar to the B5
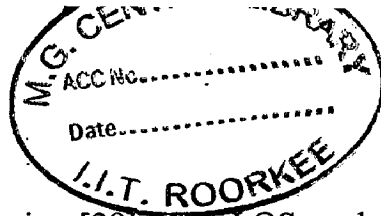
for Type F and Type G scenarios [28]. The LOS probability is expressed as a nonlinear function of the transmitter-receiver distance with cutoff points.

The time evolution behavior of mobile fading channels including transitions between different scenarios and LOS/NLOS conditions, may have a considerable impact on system performance. The SCM supports the time evolution feature based on a concept called drops [19]. A drop corresponds to a local stationary interval, during which the channel undergoes fast fading but the large-scale parameters do not change significantly. A quasi-stationary framework is used which assumes that parameters in consecutive drops are independent. The WINNER II channel model uses a concept of channel segments [22] which is similar to the concept of drops in SCM. A non-stationary framework is used to support smooth channel evolution. Transitions from an old segment to a new segment are carried out by linearly decreasing the powers of clusters in the old segment and increasing the powers of clusters in the new segment so that the old clusters are replaced one by one by the new clusters. In the SCM and WINNER II channel models, the scenario transition and LOS/NLOS transition can be simulated by changing the scenarios and LOS/NLOS conditions in consecutive drops. The IEEE 802.16j model does not explicitly address the time evolution behavior of channels.

Correlation of Multiple Links [19]- There is an environment similarity which arises from common shadowing objects and scatterers contributing to different links. This results in the dependence/ correlation of parameters describing different links. The system-level correlation is closely related to the deployment assumptions such as the heights, densities, and distances of the transmitters and receivers. A site is a highly elevated radio station, including all BSs and ART RSs. At the system level, two types of correlation can be identified: intra-site correlation and inter-site correlation. Intra-site correlation refers to the correlation between MSs connected to a site. Inter-site correlation refers to the correlation of links from a single MS to multiple sites. Both inter-site and intra-site correlations need to be considered properly in the cooperative MIMO channel model to allow accurate performance evaluation of cooperative MIMO systems.

The correlation of log normal shadow fading (SF) is perhaps the most important system level correlation because it directly influences the macro-diversity gain which is a major benefit of cooperative MIMO systems. The SF correlation is considered in all the three standardized models described in this chapter. In the SCM, the intra-site and inter-site SF correlations are fixed to 0 and 0.5 respectively. In the WINNER II model the intra-site SF correlation is a cut-off exponential decaying function of the distance between the two MSs,

25

summarized the correlation models for LSPs used in standardized MIMO channel models. We can see that these correlation models are not consistent and even contradict each other. For example, the SCM treats the intra-site SF correlation as negligible and the inter-site SF correlation as significant, while the WINNER II channel model considers the opposite. It is therefore desirable to develop a unified correlation model for LSPs. Besides the LSP correlation, the small-scale fading of multiple links in cooperative MIMO systems may also be correlated, even with largely separated antennas which need to be considered in the channel model.

3. The existing scenarios defined in the standardized MIMO channel models need to be expanded to include the M2M scenario. The M2M channel is an important type of channel in mobile user relay systems. In M2M systems both the transmitter and receiver are MSs in motion, often equipped with low-elevation antennas. M2M channels therefore differ significantly from conventional F2M channels, where only the MS is moving while the BS is fixed, often with high-elevation antennas e.g. the Doppler power spectrum density in M2M channels exhibits different shape when compared to F2M channels. The density of mobile users has a great impact on the underlying M2M channel statistics. The M2M channels in most cases are statistically non-stationary, since the stationarity conditions pertains to a much shorter time period than in F2M channels [29]. Currently, none of the existing standardized point-to-point MIMO channel models includes M2M scenarios.

Chapter 3

Chracterisation of SISO Mobile to Mobile Channel

The mobile to mobile (M2M) channel is an integral part of Cooperative MIMO systems, which involves mobile terminals. Such M2M communication channel differs from the conventional cellular radio systems, where one terminal, the BS, is stationary, and only the MS is moving. Though the received signal envelope is Rayleigh faded under NLOS, narrowband frequency flat-fading propagation conditions, the mobility of both the transmitter (Tx) and the receiver (Rx) results in different statistical properties of M2M wireless channels which was first described by Akki and Haber [11,12]. They presented a mathematical model which can be used as a reference for verifying the performance of various simulation models. The Sum-of-sinusoids (SoS) model for cellular channels was presented by Zheng and Xiao in [14,15]. The SoS model simulate a channel as a stationary, complex Gaussian random process by summing up multiple sinusoidal waveforms having carefully chosen frequencies, amplitudes, and phases to reproduce desired channel characteristics in simulations. The same SoS approach was used by Patel et. al. in [16], who proposed a statistical "double ring" scattering model to simulate the M2M channels. This chapter verifies this double ring model in terms of pdf of envelope, autocorrelation of the complex envelope, variance of the autocorrelation and level crossing rate (LCR). The results are compared with the one given in [16]. The performance of DPSK over such M2M channel is evaluated. The BER and outage probability plots are obtained and compared with the analytical results given in [30].

3.1   Mobile to Mobile Channel Modeling

A mobile radio channel may be modeled as a linear filter with a time varying impulse response, where the time variation is due to motion of Tx and Rx. In most of the practical scenarios, it is too complicated to describe the reflection, diffraction and scattering processes that determine the different multipath components. Rather, it is often preferable to describe the probability that a channel parameter attains a certain value. The stochastic channel models

29

$$R_{g_q g_q}(\tau) = E[g_q(t + \tau)g_q(t)] = J_0(2\pi f_1 \tau)J_0(2\pi f_2 \tau) \qquad (3.3)$$

$$R_{g_i g_q}(\tau) = R_{g_q g_i}(\tau) = 0 \qquad (3.4)$$

$$R_{gg}(\tau) = \frac{1}{2}E[g(t + \tau)g^*(t)] = J_0(2\pi f_1 \tau)J_0(2\pi f_2 \tau) = J_0(2\pi f_1 \tau)J_0(2\pi a f_1 \tau) \qquad (3.5)$$

where J_0 is the zero$^{\text{th}}$ order Bessel function of the first kind.

   a $= f_2/f_1$ is the ratio of the two doppler frequencies.

The autocorrelation is a product of two Bessel functions in contrast to a single Bessel function in cellular channels. The cellular channels with a=0, are a special case of M2M channels.

Doppler spectrum

The doppler spectrum [11] of such mobile-to-mobile channel is given by

$$S(f) = \frac{1}{\pi^2 f_1 \sqrt{a}} K \left[\frac{1+a}{2\sqrt{a}} \sqrt{1 - \left(\frac{f}{(1+a)f_1} \right)} \right] \qquad (3.6)$$

where $K[\cdot]$ is the complete elliptic integral [31] of the first kind which is defined as

$$K(k) = \int_0^1 \frac{dt}{\sqrt{(1 - t^2)(1 - k^2 t^2)}} \qquad (3.7)$$

the number k is called the modulus of these integrals.

The spectrum of mobile-to-mobile channels given by (3.6) differs from the U-shaped spectrum of cellular channels. The doppler spectrum, $S(f)$ has two peaks at $f = \pm(f_1 - f_2)$. The bandwidth of the spectrum is $2(1 + a)f_1$.

Level Crossing Rate (LCR) and Average Fade Duration (AFD) [16, 26]

The LCR and AFD are useful for designing error control codes and diversity schemes to be used in mobile communication systems. The LCR is the expected number of times per

31

scatter or reflect most of the transmitted energy, and will tend to modify the directivity pattern of the transmitting antenna. This results in local scattering around the Tx and the Rx, which justifies the 2-D isotropic scattering assumption in Akki and Haber's model.

In a macrocell environment, it is usually assumed that the scatterers surrounding the MS are about the same height or higher than the mobile which implies that the received signal at the mobile antenna arrives from all the directions after bouncing from the surrounding scatterers. The "single-ring" model of cellular channel, which defines scatterers as lying uniformly on a ring around the MS, can be extended to a "double-ring model". This double-ring model defines two rings of uniformly spaced scatterers around both the Tx and the Rx, thus giving rise to isotropic local scattering as illustrated in figure 3.1. The local scatterers $(1, 2, \ldots, N)$ around the
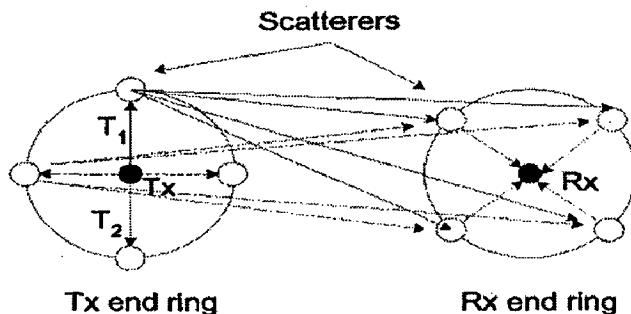

Figure 3.1 Scattering environment of mobile-to-mobile

transmitter lie on a ring of radius R_T, while the scatterers $(1, 2, \ldots, M)$ around the receiver are located on a second ring of radius R_R. The distance between the Tx and the Rx is very large compared to the radii R_T and R_R. Assuming omnidirectional antennas at both ends, the signal from the Tx antenna arrive at each of the scatterers located on the Tx end ring. Considering these scatterers as virtual BSs, the communication link from each of these scatterers to the Rx can be modeled as a conventional cellular BS-to-MS link. Hence, each "virtual BS" transmits a signal that arrives at the Rx uniformly from all directions in the horizontal plane due to isotropic scatterers located on the Rx end ring. Using this model, the narrowband complex envelope can be modeled as

$$g(t) = g_i(t) + j g_q(t) \tag{3.11}$$

33

the same amplitude i.e. there is no dominant component than the received envelope of a flat fading signal can be best modeled as being Rayleigh distributed [17]. The Rayleigh distribution is represented as

$$P_X(x) = \frac{x}{\sigma_x^2} exp\left(-\frac{x^2}{2\sigma_x^2}\right), \qquad x \geq 0 \qquad (3.16)$$

Here x is the amplitude and $\sigma_x^2 = E(x^2)$

Autocorrelation of the Complex envelope

The time-average correlations [16] of this statistical simulation model are given by following relations.

$$\hat{R}_{g_i g_i}(\tau) = \frac{1}{NM} \sum_{n,m=1}^{N,M} cos\{2\pi f_1 cos(\alpha_n)\tau + 2\pi f_2 cos(\beta_m)\tau\} \qquad (3.17)$$

$$\hat{R}_{g_q g_q}(\tau) = \frac{1}{NM} \sum_{n,m=1}^{N,M} cos\{2\pi f_1 sin(\alpha_n)\tau + 2\pi f_2 cos(\beta_m)\tau\} \qquad (3.18)$$

$$\hat{R}_{g_i g_q}(\tau) = \hat{R}_{g_q g_i}(\tau) = 0$$

$$\hat{R}_{gg}(\tau) = \frac{1}{NM} \sum_{n,m=1}^{N,M} [cos\{2\pi f_1 cos(\alpha_n)\tau + 2\pi f_2 cos(\beta_m)\tau\}$$
$$+cos\{2\pi f_1 sin(\alpha_n)\tau + 2\pi f_2 cos(\beta_m)\tau\}] \qquad (3.19)$$

Being a statistical model, its time-average correlations are random and depend on the random AOD, AOA and doppler frequencies. The conformity of these statistical properties with the mathematical reference model has been verified in the subsequent sections.

Variance of the Autocorrelation

The time-average correlations are random due to the random AODs and AOAs. Therefore, they tend to vary over simulation trials. In such a scenario, the variance defined in (3.20)

The equation (3.24) can be viewed as the conditional error probability with the condition that the γ is fixed. The average bit error rate, $P_b(E)$ in fading (γ is random) can be obtained by evaluating the following integral.

$$P_b(E) = \int_0^\infty P_b(E;\gamma)\, P_\gamma(\gamma)d\gamma \qquad (3.25)$$

Substituting (3.24) in (3.25), we get

$$P_b(E) = \int_0^\infty \frac{1}{2}exp(-\gamma)\, P_\gamma(\gamma)d\gamma \qquad (3.26)$$

The moment generating function (MGF) based approach can used to solve above integral. The MGF can be defined as

$$M_\gamma(s) = \int_0^\infty P_\gamma(\gamma)\, e^{s\gamma}\, d\gamma \qquad (3.27)$$

Using (3.26), the BER in terms of MGF can be written as

$$P_b(E) = \frac{1}{2}M_\gamma(-1) \qquad (3.28)$$

Now, for Rayleigh fading conditions, substituting (3.22) in (3.27), we get

$$M_\gamma(s) = \int_0^\infty \frac{1}{\bar{\gamma}}exp\left(-\frac{\gamma}{\bar{\gamma}}\right)\, e^{s\gamma}\, d\gamma$$

$$= \frac{1}{\bar{\gamma}}\int_0^\infty exp^{-\gamma\left(\frac{1}{\bar{\gamma}}-s\right)}d\gamma$$

$$= \frac{1}{\bar{\gamma}}\frac{\left|e^{-\gamma\left(\frac{1}{\bar{\gamma}}-s\right)}\right|_0^\infty}{-\left(\frac{1}{\bar{\gamma}}-s\right)}$$

$$= \frac{1}{-(1-s\bar{\gamma})}(0-1) = \frac{1}{(1-s\bar{\gamma})} \qquad (3.29)$$

37

3.3.1 PDF of the Mobile to Mobile Channel

The angles θ and Ψ required in equations (3.14, 3.15) are randomly generated from a uniform distribution over interval $[-\pi, \pi)$. The AOD, α_n and AOA, β_m are calculated for each (N,M) pair using equations (3.14, 3.15). Thereafter, the in phase and quadrature phase channel coefficients, $g_i(t)$ and $g_q(t)$ are discretely generated for each time instant using equations (3.12, 3.13). The summation is implemented by running two loops (N and M times). The channel coefficient, $g(t)$ for each time instant is calculated using (3.11). With a sampling rate of 10^{-3} s and simulation time of 50 s, we get a total of 50000 samples of channel coefficients.

Since the variance (σ^2) of the in phase and quadrature phase of channel coefficients is unity, the range of amplitudes is defined from -5 to 5, with interval 0.125 resulting in 80 intervals. Total number of observations of $g_i(t)$, $g_q(t)$ and $|g(t)|$ falling in each interval are calculated and stored. The averaging of number of observations obtained in each interval is carried out, over 50 trials. The histogram approach is used to obtain the plots of pdfs of $g_i(t)$, $g_q(t)$ and $|g(t)|$. The normalization is done so as to ensure the area under the curve as unity.

The analytic plots for the pdf of $g_i(t)$, $g_q(t)$ and $|g(t)|$ are also obtained using (3.16). The simulation and analytic plots of pdfs of in-phase and quadrature phase components of channel coefficient are show in figure 3.2(a) and 3.2(b) respectively. Both the plots coincide with each other and have Gaussian distribution with zero mean and unit variance. The analytic and simulated results for the pdf of $|g(t)|$ are shown in figure 3.2(c). The variance of distribution of $|g(t)|$ is found to be $(2 - \pi/2)$ which is close to the theoretical value of Rayleigh pdf. The pdf curve peaks at unit amplitude with the peak value of probability density being 0.6. It is observed that pdf of amplitude of channel coefficients derived from simulation is very close to the Rayleigh pdf with reasonable number of scatterers, i.e. $N = M = 12$.

3.3.2 Autocorrelation of the Complex envelope

The channel coefficients of double ring channel model are simulated using the procedure given in section 3.1.1. With a sampling rate of 10^{-4} s and simulation time of 0.1 s, we get a total of 1000 samples of channel coefficients. The library function "xcorr" available in MATLAB is used to calculate the time averaged autocorrelation of the channel coefficients. The simulation results are averaged over 100 trials. The autocorrelation is also directly simulated using equation (3.19). The corresponding plot for the mathematical reference model is obtained by using (3.5).

Figure 3.3 plots the autocorrelation of the simulated double ring model (both direct simulation of the autocorrelation relation and correlation of the simulated channel coefficients) and compares it with the autocorrelation of the reference model. For the normalized time-delay range, $(0 \leq f_1\tau \leq 3)$, which is typically of interest for most communication systems, the double ring channel model provides a good approximation to the desired autocorrelation.

3.3.3 Variance of the Autocorrelation

The angles θ and Ψ required in equations (3.14, 3.15) are randomly generated from a uniform distribution over interval $[-\pi, \pi)$. The AOD, α_n and AOA, β_m are calculated for each (N,M) pair using equations (3.14, 3.15). The time-average autocorrelation at discrete interval is calculated for each time instant, using (3.19) and given simulation parameters except the number of scatterers on Tx and Rx end ring, which are considered as 8. The summation is implemented by running two loops (N and M times). We get total 1000 samples of autocorrelation. The autocorrelation of the complex envelope for the mathematical reference model is also calculated by using (3.5). The variance of the autocorrelation of the statistical model is evaluated by averaging the squared error in correlations given by (3.20) over 500 trials. The corresponding variance for Akki and Haber's simulation model are obtained by using (3.21). For a fair comparison, we used $N=64$ sinusoids in Akki and Haber's simulation model, which is equal to $N \times M=64$ sinusoids used for the two ring model. The variance of two ring model and the Akki and Haber's simulation model is compared in figure 3.4, which shows that the variance of the two ring simulation model is considerably lower than that of Akki and Haber's simulation model.
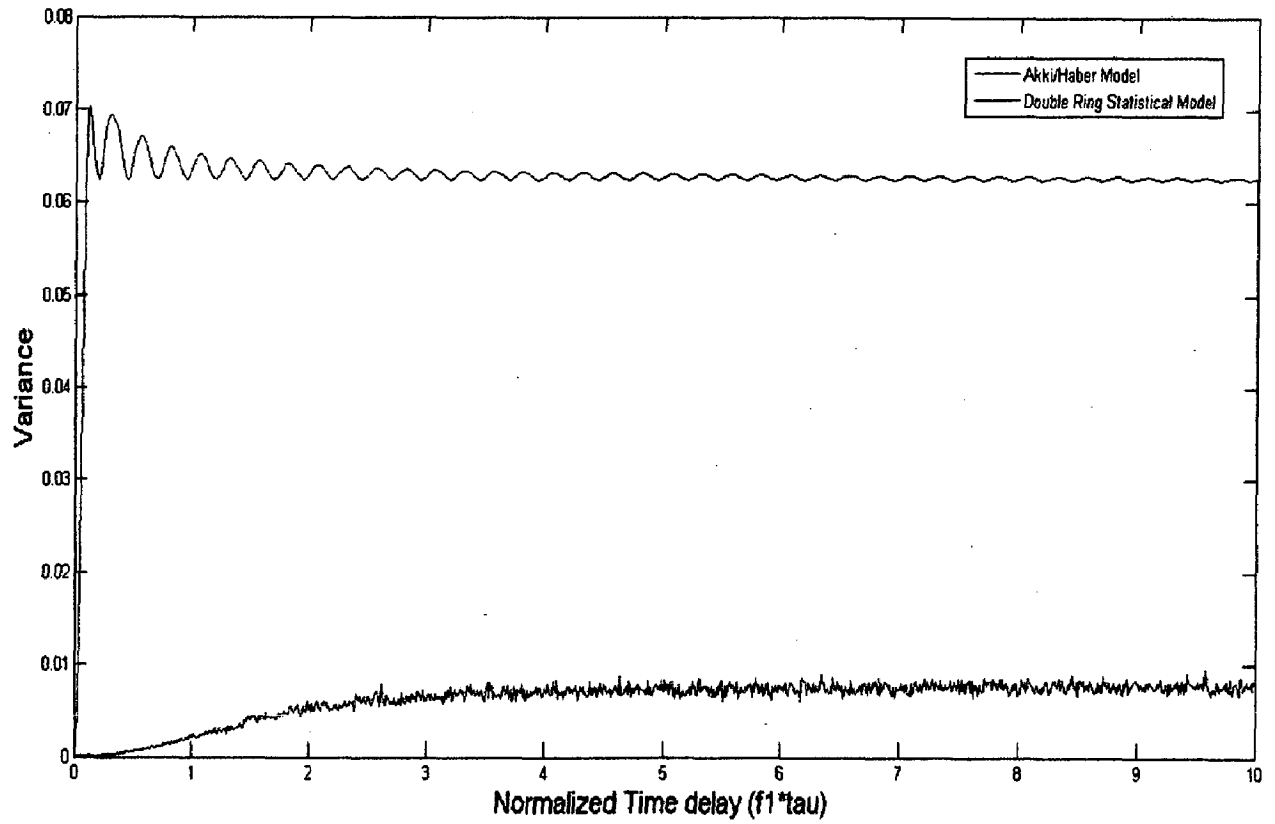
Figure 3.4 Variance of the Autocorrelation of Mobile-to-mobile channel

43

3.3.5 BER of DPSK over Single Rayleigh Channel

The fading channel coefficients of double ring channel model are simulated using the procedure given in section 3.1.1. The zero doppler is assumed in simulations in order to have fair comparison with the analytical results of BER of DPSK over single Rayleigh Channel. With a sampling rate of 10^{-3} s and simulation time of 400 s, we get total 400000 samples of channel coefficients.

Random binary sequence $\{b_k\}$ is generated using library function rand(). The differential encoding process starts with the arbitrary first bit and the differentially encoded sequence $\{d_k\}$ is generated using the logical relation

$$d_k = d_{k-1}b_k + \bar{d}_{k-1}\bar{b}_k \quad \text{modulo 2} \qquad (3.33)$$

Since binary transmission is considered, the phase assigned is $0°$ or $180°$ and the modulated signal consists of real signals '1' or '-1'. This transmitted sequence is multiplied with the channel coefficients and thereafter, the complex Gaussian noise with variance corresponding to SNR in the range (2 db to 35 db) is added. At receiver, the phase of the received signal at current time instant is compared with its phase in the previous time instant. If this phase difference is more than $90°$, it is considered as change of phase and decoded as '-1' or else it is considered "no phase change" and decoded as '1'. This logic results in differential decoding of the received signal. Numbers of errors are determined by comparing the decoded sequence with the data sequence before encoding. The BER is calculated by dividing the number of errors by the total number of bits, i.e. 400000. The BER is calculated for each value of SNR. Total 100 experiments are carried out and the bit error rates are averaged over these trials. The theoretical value of BER corresponding to each SNR value is obtained by using equation (3.30). The comparison of the plots of simulated and analytic BER versus SNR in db is shown in figure 3.6. It may be seen that the simulated curve closely follows the analytic curve over entire range of SNRs.

3.2.6 Outage probability

The fading channel coefficients of double ring channel model are simulated using the procedure given in section 3.1.1. The zero doppler is assumed in simulations in order to have fair comparison with the analytical results of Outage probability over Single Rayleigh Channel. The instantaneous SNR is calculated by using the following relation.

$$\gamma_{inst} = \frac{\alpha^2}{\text{noise variance}} \qquad (3.34)$$

where α is the amplitude of channel coefficient. The threshold SNR, γ_{th} is considered as 0 db. The range of SNR (E_b/N_o) considered is 0 db to 32 db with step size of 1 db. The outage probability for each value of SNR is evaluated by comparing the γ_{inst} with γ_{th}. Whenever instantaneous SNR falls below threshold, it is considered as outage event. Total 20000 simulation trials were run and results were averaged out. The analytic results are obtained by using the equation (3.32). The simulated and analytic plots of outage probability versus SNR are shown in figure 3.7. It may be seen that the simulated curve closely follows the analytic curve upto SNR of 24 db which corresponds to outage probability of 2×10^{-3}. The conformity of the curves will further improve if more number of trials are carried out.

Chapter 4

Chracterisation of Cooperative MIMO Channel

In a cooperation diversity scheme, one MS partners with another MS to send (or receive) its signal to (from) the base station (BS) or some other final destination. The partner station serves as a relay, forwarding the signal from the source to the destination. This provides receive or transmit antenna diversity in a virtual fashion, depending on whether the link is downlink or uplink. Such a cooperative system promises to increase the system capacity and coverage. This concept of virtual diversity is the basis of Cooperative MIMO technology.

The single relay acting as Amplify and Forward (A & F) node forms the simplest scenario for cooperative communication. The concept of double ring model is extended to simulate this relay channel as three ring model, in which the ring of scatterers is also considered around the relay node. Under flat fading conditions, the overall channel from the source to the destination via the relay in A & F systems is "double Rayleigh" with properties quite different from a typical cellular channel. This chapter verifies this three ring model in terms of statistical properties such as the envelope probability density function, autocorrelation, level crossing rate and doppler spectrum. The results are compared with the theoretical plots, wherever analytic relations are available. The performance of DPSK over such a relay channel is evaluated. The BER and outage probability plots are obtained and compared with the analytical results given in [9,10].

In diversity combining, two or more copies of same information-bearing signal are combined skillfully to increase the overall SNR. The Maximum Ratio Combining (MRC) is considered, to study the multichannel cooperative diversity (CD) networks. Closed form expressions of BER and outage probability for such cooperating networks cannot be derived. Therefore, the M2M channel model described in chapter 2 is extended to simulate such CD networks. The simple case of one cooperating terminal with a direct and relayed path is simulated. The plots of BER and outage probability of BPSK over this two path network are obtained and compared with the results given in [18]. Finally, the CD network having five

where $s(t)$ is the transmitted signal with average power E_1

$g_1(t)$ is the channel gain between the mobile terminal A and the relay modeled as a wide-sense stationary (WSS) zero mean complex Gaussian random (ZMCG) process with power σ_1^2.

and $n_1(t)$ is complex additive white Gaussian noise (AWGN) with power σ_n^2

The relay amplifies $r_1(t)$ and retransmits it to the destination MS which receives

$$
\begin{aligned}
r_2(t) &= A(t)\, g_2(t)\, r_1(t) + n_2(t) \\
&= A(t)\, g_2(t)\, g_1(t)\, s(t) + A(t)\, g_2(t)\, n_1(t) + n_2(t) \\
&= g(t)\, s(t) + A(t)\, g_2(t)\, n_1(t) + n_2(t)
\end{aligned}
\qquad (4.2)
$$

where $A(t)$ is the amplification factor scaling the power transmitted by the relay

$g_2(t)$ is the channel gain between the relay and the destination MS, modeled as a WSS ZMCG process with power $\sigma_2{}^2$

$g(t) = A(t)\, g_1(t)\, g_2(t)$ is the overall relay channel

and $n_2(t)$ is zero mean complex AWGN with power σ_n^2.

Here, we assume that the relay and the destination receiver chains have identical noise properties and, hence the same AWGN power. In the subsequent discussion, the time index t is dropped for convenience while remembering that all the random processes involved are WSS. The amplification factor A can have several different choices out of which following two have been analyzed in [17]

$$
A_1 = \sqrt{\frac{E_2}{E[|r_1|^2]}} = \sqrt{\frac{E_2}{E_1 \sigma_1^2 + \sigma_n^2}}
\qquad (4.3)
$$

$$
A_2 = \sqrt{\frac{E_2}{E_2 |g_1|^2 + \sigma_n^2}}
\qquad (4.4)
$$

Here, E_2 denotes the average power transmitted by the relay. The gain A_1 in (4.3) requires the knowledge of the average power received by the relay while the gain A_2 in (4.4) requires the relay to have instantaneous channel knowledge g_1. The relays with gain A_1 using a constant

Time-Domain Correlations

Consider isotropic antennas operating in a two-dimensional (2-D) isotropic scattering environment corresponding to non-line-of-sight (NLOS) conditions at the source MS, relay station and destination MS. This assumption is justified by the low elevation of the source, relay and destination terminals. The auto-correlation can be derived as

$$R_{gg}(\tau) = \frac{1}{2}E[g(t+\tau)g^*(t)]$$

$$= \frac{1}{2}E[g_1(t+\tau)g_2(t+\tau)g_1^*(t)g_2^*(t)] \qquad (4.8)$$

Since g_1 and g_2 are independent, (4.8) reduces to

$$R_{gg}(\tau) = \frac{1}{2}E[g_1(t+\tau)g_1^*(t)]E[g_2(t+\tau)g_2^*(t)]$$

$$= 2R_{g_1 g_1}(\tau)\,R_{g_2 g_2}(\tau)$$

Substituting the autocorrelation value of g_1 and g_2 obtained from Akki and Haber's mobile-to-mobile channel model, given in (3.5).

$$R_{gg}(\tau) = 2\left\{\frac{\sigma_1^2}{2}J_0(2\pi f_1 \tau)\,J_0(2\pi f_2 \tau)\right\}\left\{\frac{\sigma_2^2}{2}J_0(2\pi \widehat{f_2}\tau)\,J_0(2\pi f_3 \tau)\right\}$$

$$= \frac{\sigma_1^2 \sigma_2^2}{2}J_0(2\pi f_1 \tau)\,J_0(2\pi f_2 \tau)\,J_0(2\pi \widehat{f_2}\tau)\,J_0(2\pi f_3 \tau) \qquad (4.9)$$

where $J_0(x)$ is the zero[th] order Bessel function of the first kind

f_1 and f_2 are the maximum Doppler shift induced by the motion of the source and the relay respectively, in the source-relay link having wavelength λ_1.

$\widehat{f_2}$ and f_3 are the maximum Doppler shift induced by the motion of the relay and the destination MS respectively, in the relay-destination link having wavelength λ_2.

The carrier frequencies used in the source-relay link and the relay-destination link may be either same or different. Using the time division multiple access (TDMA) based multi-access protocol, the two carrier frequencies are same, thereby implying $f_2 = \widehat{f_2}$. This assumption yields the simplified autocorrelation function as

$$= \frac{E_2 |g_1|^2 |g_2|^2 E_1}{E_2 |g_2|^2 \sigma_n^2 + \sigma_n^2 E_1 \sigma_1^2 + \sigma_n^2 \sigma_n^2}$$

$$= \frac{\gamma_1 \gamma_2}{\gamma_2 + \overline{\gamma_1} + 1} \qquad (4.13)$$

where $\gamma_i = E_i |g_i|^2 / \sigma_n^2$ is the instantaneous SNR of the ith individual channel (or i^{th} hop) with an average SNR value $\overline{\gamma_i} = E_i \sigma_i^2 / \sigma_n^2$.

For variable gain relays having gain A_2 defined in (4.4), the equivalent SNR [10] at the receiver is given by:

$$\gamma_{eq} = \frac{\gamma_1 \gamma_2}{\gamma_1 + \gamma_2 + 1} \qquad (4.14)$$

The choice of the above gain aims to limit the output power of the relay if the fading parameter of the first channel, $\alpha_1 = |g_1|$ is low. The form of the equivalent SNR in (4.14) is not easily tractable due to the complexity in finding the statistics (i.e., the PDF, CDF, and MGF) associated with it. Fortunately, this form can be tightly bounded by

$$\gamma_{eq}' = \frac{\gamma_1 \gamma_2}{\gamma_1 + \gamma_2} \qquad (4.15)$$

The form has the advantage of mathematical tractability over that in (4.14) in addition to be a tight upper bound, specially at high average SNR. This will later translate to a tight lower bound when talking about average bit-error rate (BER) and outage probability performance criteria. It can be seen from (4.15) that γ_{eq}' is half of the harmonic mean $\mu_H(\gamma_1, \gamma_2)$. Since the two channels (source to relay and relay to destination) are individually Rayleigh distributed, the SNRs γ_1 and γ_2 are exponentially distributed with following pdfs.

$$p_{\gamma_1}(\gamma_1) = \frac{1}{\overline{\gamma_1}} exp\left(-\frac{\gamma_1}{\overline{\gamma_1}}\right) \quad , \gamma_1 \geq 0 \qquad (4.16)$$

$$p_{\gamma_2}(\gamma_2) = \frac{1}{\overline{\gamma_2}} exp\left(-\frac{\gamma_2}{\overline{\gamma_2}}\right) \quad , \gamma_2 \geq 0 \qquad (4.17)$$

The MGF based approach has been used in [10] to derive the PDF of γ_{eq}' which is given as

If the two links are identical, i.e. $\bar{\gamma}_1 = \bar{\gamma}_2 = \bar{\gamma}$, , then the MGF in (4.19) reduces to

$$M_{\gamma'_{eq}}(s) = {}_2F_1\left(1,2\,;\,\frac{3}{2}\,;\,\frac{-\bar{\gamma}}{4}s\right)$$

which can be written in terms of the more common inverse hyperbolic sin function as

$$M_{\gamma'_{eq}}(s) = \frac{\sqrt{\frac{\bar{\gamma}}{4}s\left(\frac{\bar{\gamma}}{4}s+1\right)} + \text{arcsinh}\left(\sqrt{\frac{\bar{\gamma}}{4}s}\right)}{2\sqrt{\frac{\bar{\gamma}}{4}s}\left(\frac{\bar{\gamma}}{4}s+1\right)^{3/2}} \qquad (4.20)$$

The BER for binary DPSK in terms of MGF is already derived in section 3.2, which is reproduced below.

$$P_b(E) = \frac{1}{2}M_\gamma(-1) \qquad (4.21)$$

The BER for DPSK over the relay channel can be obtained by substituting (4.20) in (4.21), which reduces to:

$$P_b(E) = \frac{\sqrt{-\frac{\bar{\gamma}}{4}\left(-\frac{\bar{\gamma}}{4}+1\right)} + \text{arcsinh}\left(\sqrt{-\frac{\bar{\gamma}}{4}}\right)}{4\sqrt{-\frac{\bar{\gamma}}{4}}\left(-\frac{\bar{\gamma}}{4}+1\right)^{3/2}} \qquad (4.22)$$

The outage probability for the relay channel can be derived by substituting the pdf of overall SNR (γ'_{eq}) in the definition of outage probability (3.31). The resultant simplified expression is given in [10], which is replicated below.

$$P_{out} = 1 - \frac{2\,\gamma_{th}}{\sqrt{\bar{\gamma}_1\bar{\gamma}_2}}K_1\left(\frac{2\gamma_{th}}{\sqrt{\bar{\gamma}_1\bar{\gamma}_2}}\right)exp^{-\gamma_{th}\left(\frac{1}{\bar{\gamma}_1}+\frac{1}{\bar{\gamma}_2}\right)} \qquad (4.23)$$

In (4.23), the predetermined protection ratio γ_{th} is a threshold SNR above which the quality of service is satisfactory and which essentially depends on the type of modulation employed and the type of application supported. The above stated analytical expression of BER and outage probability are valid only under tight assumptions like high average SNR and the average SNRs of two links being identical. These assumptions might not be true in practical scenarios.

57

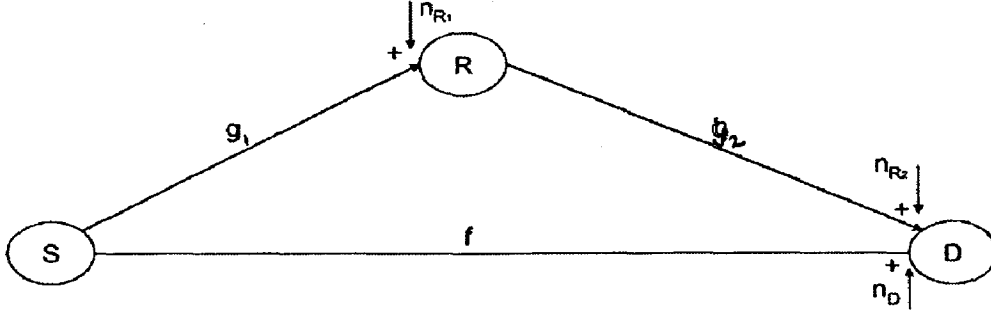signal through the complex channels S-R and R-D with flat-fading coefficients g_1 and g_2, respectively.

Figure 4.3 Two branch CD network

It is assumed that all the additive white Gaussian noise (AWGN) terms n_{R_1}, n_{R_2} and n_D have equal variance N_0. The Amplify and Forward (AF) model for the relay is considered. Assuming that direct and relay path are orthogonal channels, the destination D receives two independent copies of the signal, s transmitted by the source

$$y_D = fs + n_D \tag{4.24}$$

$$y_R = g_2 A (g_1 s + n_{R_1}) + n_{R_2} = g_2 A g_1 s + n_R \tag{4.25}$$

where $n_R = g_2 A n_{R_1} + n_{R_2}$ and A is the amplification factor of the relay. The receiver collects these copies with a maximum ratio combiner (MRC). The noise terms n_R and n_D do not have identical power because n_R also includes a noise contribution at the intermediate stage. Therefore, the MRC is preceded by a noise normalization step. This combining rule is used to form a decision variable, z.

$$z = \left(\frac{f}{\sigma_D}\right)^* y_D + \left(\frac{g_2 A g_1}{\sigma_R}\right)^* y_R \tag{4.26}$$

whose SNR is given by

$$\gamma_z = |f|^2 \frac{E_s}{\sigma_D^2} + |A g_1 g_2|^2 \frac{E_s}{\sigma_R^2} = \gamma_D + \gamma_R \tag{4.27}$$

$$\gamma_z = \frac{\gamma_{g_1}\gamma_{g_2}}{\gamma_{g_1} + \gamma_{g_2}} + \gamma_D \qquad (4.32)$$

The similar approach has been used in [18] to derive the following equivalent SNR relation for the general case of K cooperating terminal network, having $K+1$ branches.

$$\gamma_z = \gamma_D + \sum_{i=1}^{K} \frac{\gamma_{g_{1i}}\gamma_{g_{2i}}}{\gamma_{g_{1i}} + \gamma_{g_{2i}}} \qquad (4.33)$$

where g_{1i} and g_{2i} are the channel coefficients for each of the $i=1,2.....K$ branches with relays, corresponding to S to R and R to D link respectively.

The closed form expression for BER over such cooperative networks cannot be obtained. However, the average BER for sufficiently large SNR is evaluated in [18] by looking at the pdf of the SNR around zero. The BER for BPSK over such Rayleigh fading channel has been approximated with the following analytic relation.

$$P_b(E) \approx \frac{3}{16}\left(\frac{1}{\gamma_{g_1}} + \frac{1}{\gamma_{g_2}}\right)\frac{1}{\gamma_D} \qquad (4.34)$$

4.3   Simulation Results

The single relay channel and multi-branch CD networks have been simulated by using the mobile to mobile double ring model (3.11 to 3.15) for each link and the MRC rule given in (4.26). Unless stated otherwise, the following parameters have been used in all simulations.

Number of scatterers located around each terminal = 12

Average transmitted power = 1

Doppler frequencies, $f_1 = f_2 = f_3 = 100$ Hz

Sampling Period = 10^{-3} s

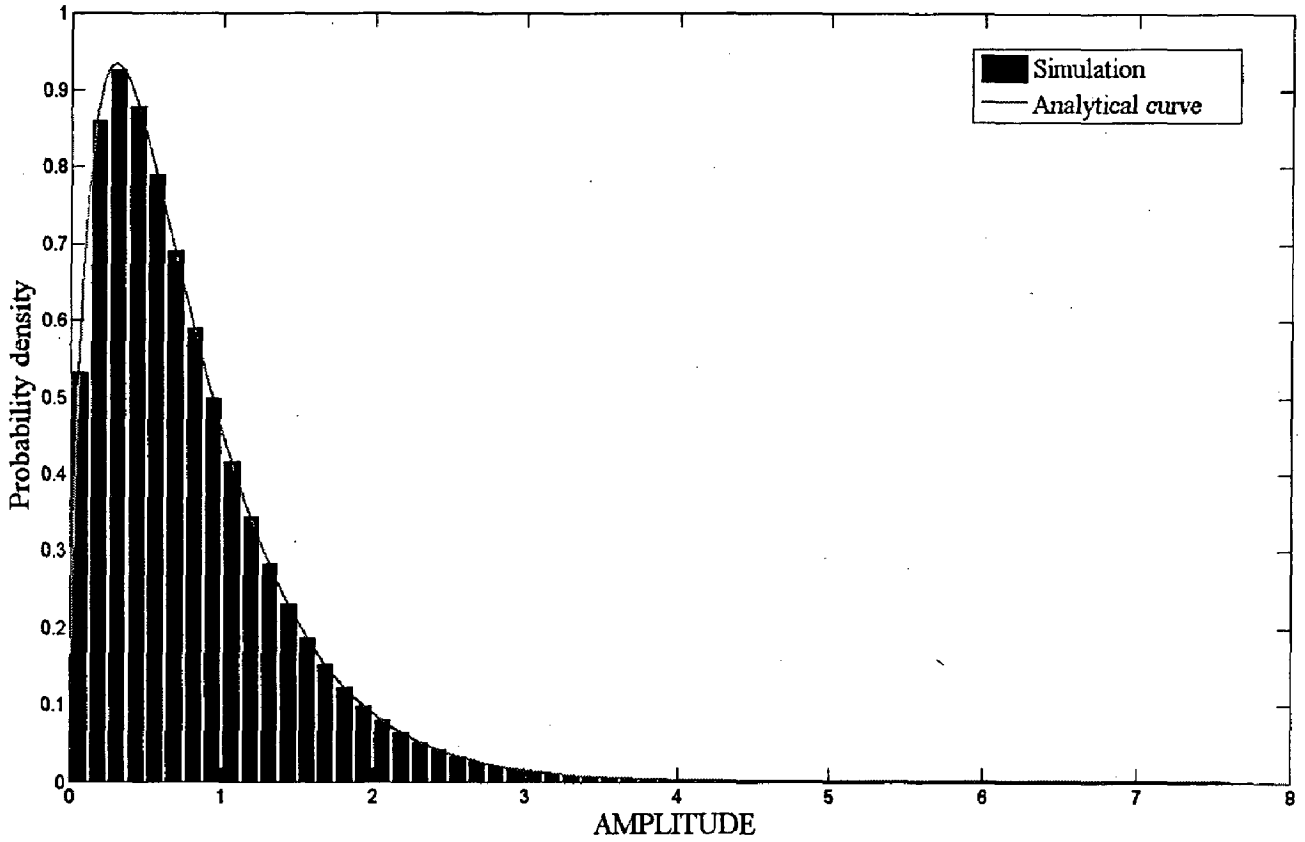Simulation time = 50 s

Number of trials = 50

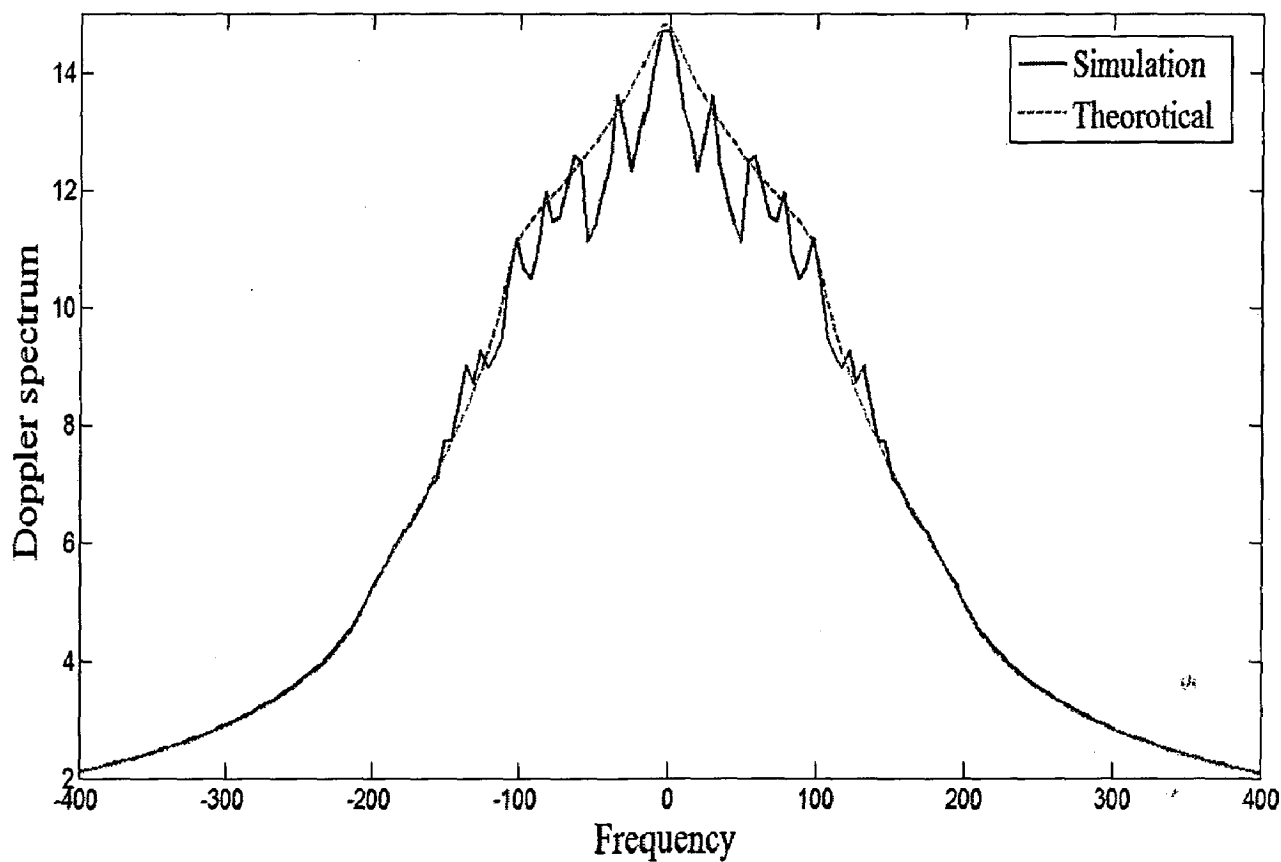Figure 4.4   PDF of the complex envelope of double Rayleigh channel

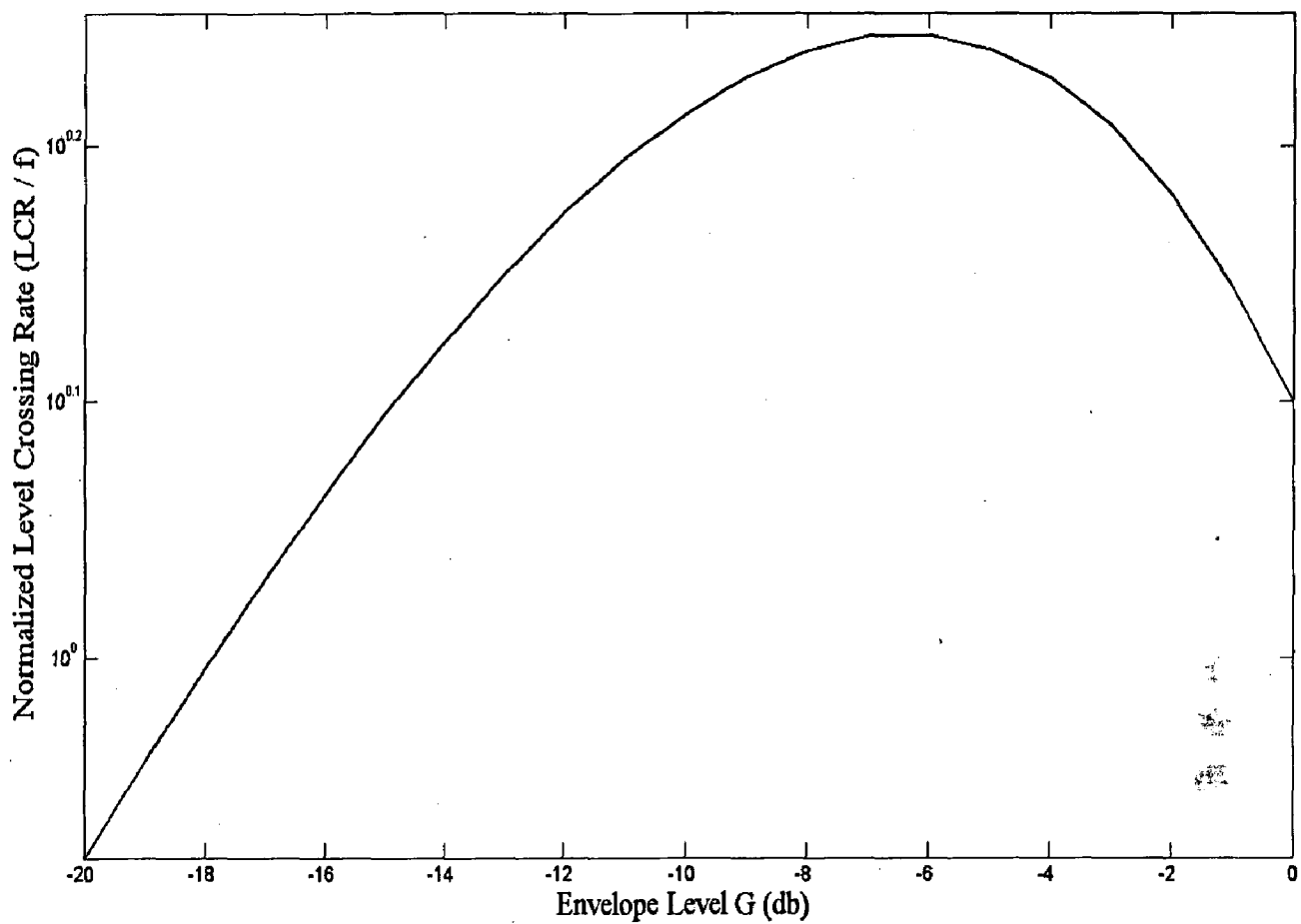Figure 4.6   Doppler spectrum of the double Rayleigh channel

65

Figure 4.7 Level crossing rate of the double Rayleigh channel
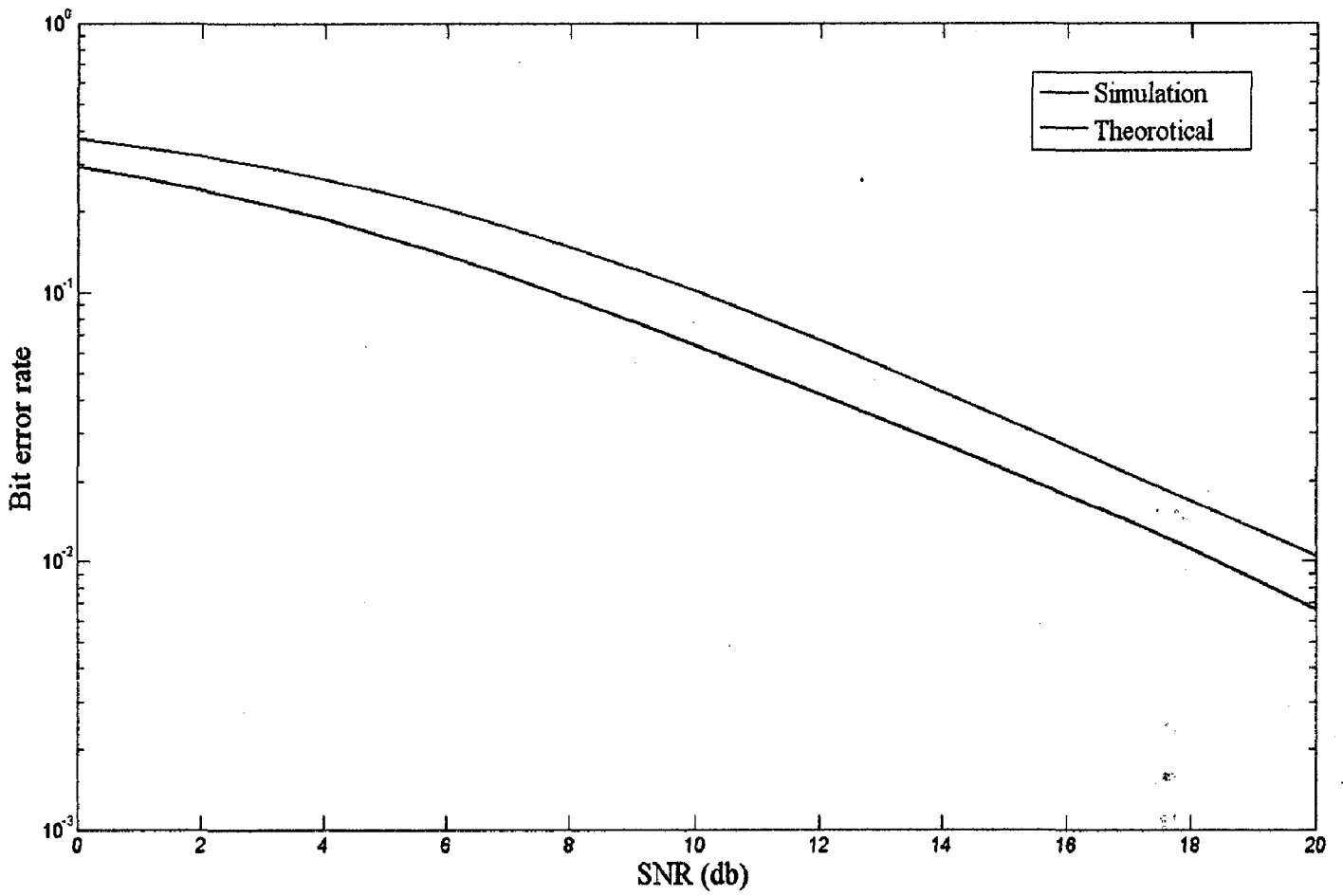
Figure 4.8 BER of DPSK over double Rayleigh channel

4.3.5 Simulation of Multibranch CD networks

The three mobile to mobile links of single cooperating terminal network shown in figure (4.3) are simulated and 200000 samples of channel coefficients, g_1, g_2 and f are generated as per the given procedure. The complex gaussian noise n_{R_1}, n_{R_2} and n_D are generated with variance corresponding to SNR in the range (1 db to 20 db). The uniformly distributed BPSK sequence of '1' and '-1' is generated using library function rand(). Equations (4.24) and (4.25) are used to calculate the received signal in the direct and relayed path respectively. These signals are combined as per equation (4.26), so as to generate the decision variable, z. If the real part of $z > 0$, the received signal is detected as '1' or else '-1'. Numbers of errors are determined by comparing the decoded sequence with the data sequence before encoding. The BER is calculated by dividing the number of errors by the total number of bits in the sequence. The BER is calculated for each value of SNR. Total 100 experiments are carried out and the bit error rates are averaged over these trials. The BER is also calculated individually for the direct and relayed path. These plots of BER Vs SNR are shown in figure 4.10. It may be seen that the BER for cooperative scenario is lesser than direct and relayed path, over entire range of SNRs. The performance of relayed path is worst because of the double Rayleigh fading encountered in that path.

The same approach is used to simulate the multipath CD network and the BERs are calculated for the combination of two, three, four and five branches. These plots are shown in figure 4.11. The comparison of these plots clearly brings out the diversity gain associated with the multibranch cooperation.
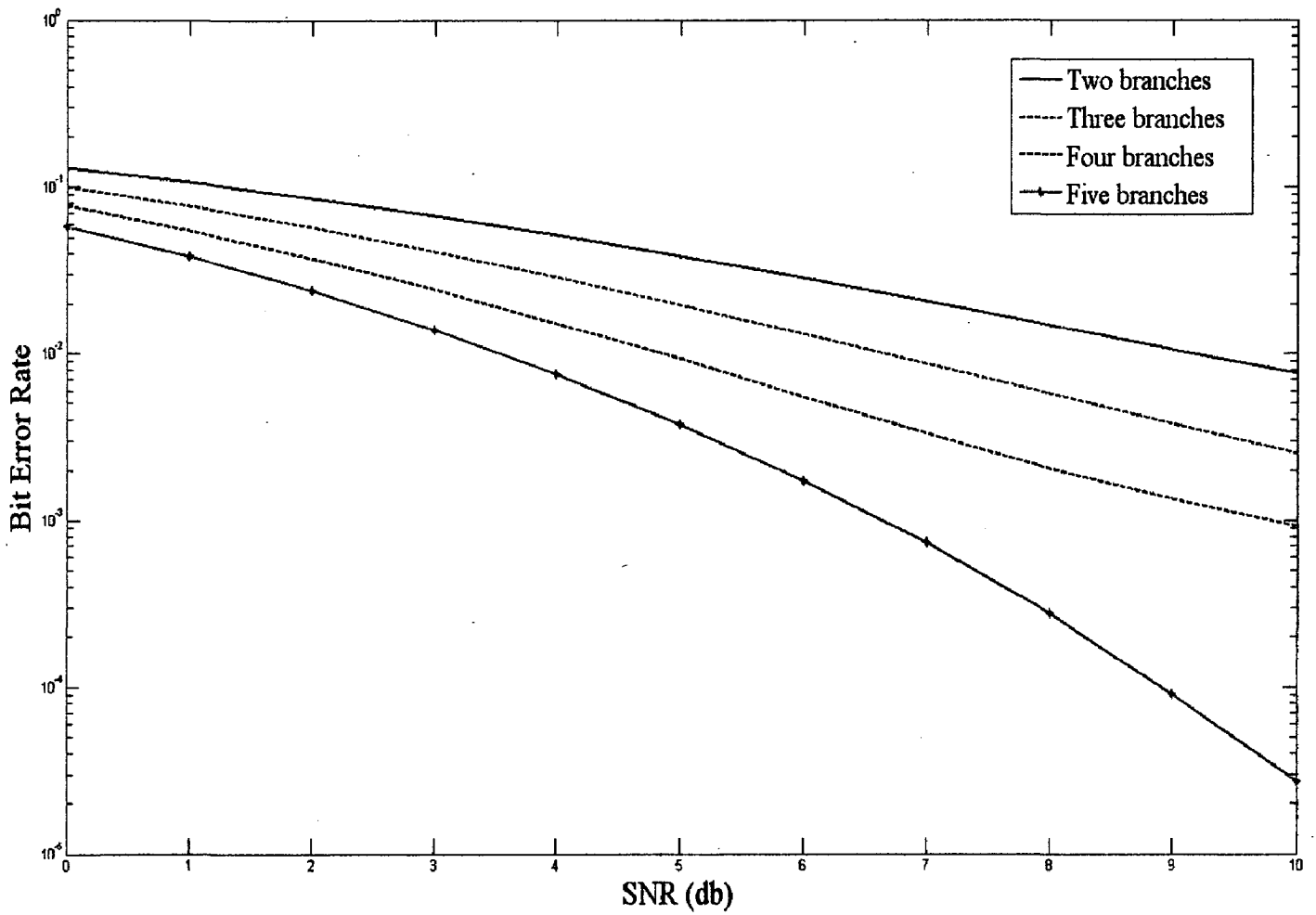
71

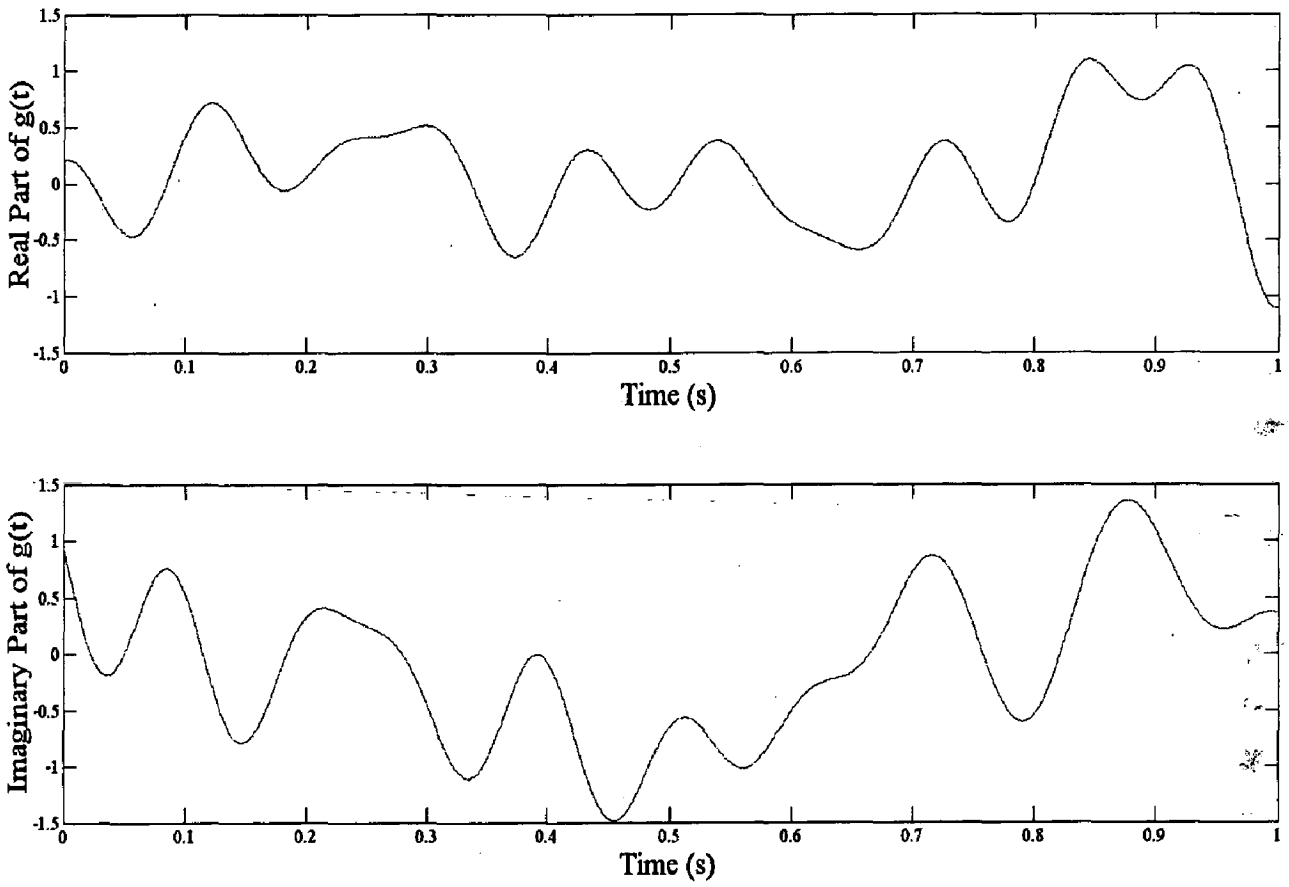Figure 4.11 BER of BPSK over Multibranch CD network

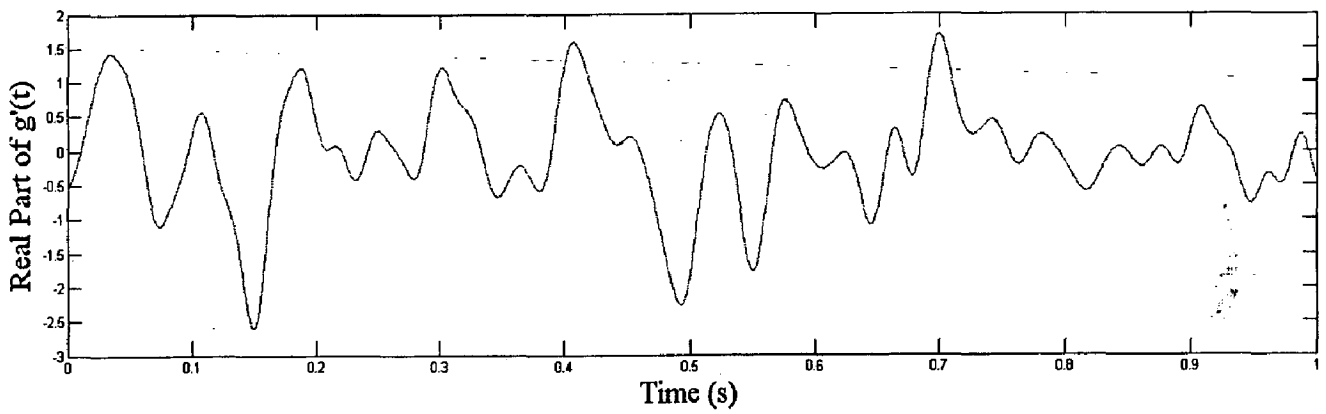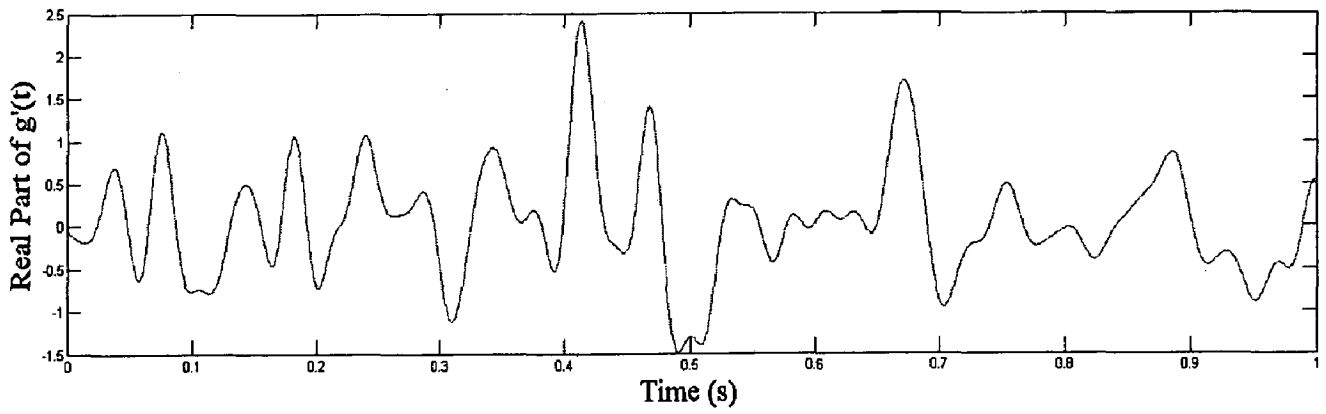Figure 4.12 Time variation of single Rayleigh channel with doppler frequency of 10 Hz

Figure 4.14 Time variation of double Rayleigh channel with doppler frequency of 10 Hz

Chapter 5

Conclusion

The high data rates offered by Cooperative MIMO technology makes it most eligible candidate for forthcoming 4G cellular systems which can support high speed applications on the mobile networks. The realistic cooperative MIMO channel models are indispensable to accurately evaluate and compare the performance of different transmission technologies for cooperative MIMO systems. This thesis explores the modeling approach for such cooperative MIMO channels. The tapped delay model of MIMO channel is presented before giving an insight to standardized point to point MIMO channel models like WINNER II, 3GPP SCM, SUI and IEEE 802.16j channel model. Out of these models, the WINNER II seems to be most versatile which provides a pool of 13 different scenarios. In spite of their versatility, the existing standardized point-to-point MIMO channel models are inadequate to provide a complete model for cooperative MIMO channels. This motivates to look for the statistical simulation model for such channels.

The mobile to mobile (M2M) channel is an integral part of Cooperative MIMO systems. The Akki and Haber's mathematical reference model for M2M channel is presented which is used as a reference for verifying the performance of simulation model. The "double-ring" scattering model proposed by Patel et. al. uses sum-of-sinusoids approach which simulates a channel as a stationary, complex Gaussian random process by summing up multiple sinusoidal waveforms having carefully chosen frequencies, amplitudes, and phases to reproduce desired channel characteristics. This double ring model with 12 scatterers around each terminal is used to simulate M2M channel. Various statistical properties like pdf of complex envelope, autocorrelation, variance of the autocorrelation and level crossing rate (LCR) are evaluated which confirms with the mathematical reference model. The performance of DPSK in terms of BER and outage probability over such M2M channel is evaluated and compared with the available analytical results.

The single relay acting as Amplify and Forward (A & F) node forms the simplest scenario for cooperative communication. The statistical properties like time domain correlation, doppler spectrum, level crossing rate and signal to noise ratio of the fixed gain relay channel are elaborated which provides understanding about the characteristics of the

References

[1] Arogyaswami J Paulraj, Dhananjay Gore, Rohit Nabar and Helmut Bolcskei, "An Overview of MIMO Communications—A Key to Gigabit Wireless", *Proceedings of the IEEE*, vol. 92, no. 2, pp 198-218, Feburary 2004.

[2] A. Sendonaris, E. Erkip, and B. Aazhang, "User cooperation diversity- Part I: System description", *IEEE Transactions on Communication*, vol. 51, no. 11, pp. 1927–1938, Nov. 2003.

[3] A. Sendonaris, E. Erkip, and B. Aazhang, "User cooperation diversity-Part II: Implementation aspects and performance analysis", *IEEE Transactions on Communication*, vol. 51, no. 11, pp. 1939–1948, Nov. 2003.

[4] A. Nosratinia, T.E. Hunter, A. Hedayat, "Cooperative communication in wireless networks", *IEEE Communications Magazine*, vol. 42, no.10, pp. 74- 80, Oct. 2004.

[5] J.N. Laneman, D.N.C. Tse and G.W. Wornell , "Cooperative diversity in wireless networks: Efficient protocols and outage behavior", *IEEE Transactions on Information Theory*, vol. 50, no. 12, pp. 3062- 3080, Dec. 2004.

[6] T.E. Hunter, A. Nosratinia, "Cooperation diversity through coding", *IEEE International Symposium on Information Theory*, Lausanne, Switzerland, pp. 220, July 2002.

[7] T.E. Hunter, A. Nosratinia, "Diversity through coded cooperation", *IEEE Transactions on Wireless Communications*, vol. 5, no. 2, pp. 283- 289, Feb. 2006.

[8] J. Salo, H. M. Sallabi, P. Vainikainen, "The distribution of the product of independent Rayleigh random variables", *IEEE Transactions on Antennas and Propagation*, vol. 54, no. 2, pp. 639- 643, Feb. 2006.

[9] M. O. Hasna and M. S. Alouini, "A performance study of dual-hop transmissions with fixed gain relays", *IEEE Transactions on Wireless Communications*, vol. 3, no. 6, pp. 1963–1968, Nov. 2004.

[20] T.D. Nguyen, O. Berder, O. Sentieys, "Cooperative MIMO Schemes Optimal Selection for Wireless Sensor Networks", *IEEE Vehicular Technology Conference (VTC 2007-Spring)*. pp. 85-89, 22-25 April 2007.

[21] 3GPP TR 25.996, "Spatial Channel Model for Multiple Input Multiple Output (MIMO) Simulations (Rel. 6)", Sept. 2003.

[22] P. Kyosti *et. al.*, "WINNER II Channel Models," IST-WINNER II D1.1.2, Nov. 2007.

[23] Arogyaswami Paulraj, Rohit Nabar and Dhananjay Gore, *Introduction to Space-Time Wireless Communications*, Cambridge University Press, 2006.

[24] John G. Proakis, *Digital Communication*, McGraw Hill, Fourth Edition, 2000.

[25] P. Almers, E. Bonek, A. Burr, N. Czink and M. Debbah, "Survey of Channel and Radio Propagation Models for Wireless MIMO Systems", *EURASIP Journal on Wireless Communications and Networking*, Vol. 2007, Article ID: 19070, 2009.

[26] T. Rappaport, *Wireless Communications, Principles and Practice*, Prentice-Hall, Englewood Cliffs, NJ, USA, 1996.

[27] C.-X. Wang, X. Cheng, and D. I. Laurenson, "Vehicle to Vehicle Channel Modeling and Measurements: Recent Advances and Future Challenges", *IEEE Communication Magazine*, vol. 47, no. 11, pp. 96–103, Nov. 2009.

[28] G. Senarth *et al.*, "Multi-hop Relay System Evaluation Methodology (Channel Model and Performance Metric)", IEEE 802.16j-06/013r3, Feb. 2007.

[29] C. X. Wang *et. al.*, "Spatial Temporal Correlation Properties of the 3GPP Spatial Channel Model and the Kronecker MIMO Channel Model", *EURASIP Journal on Wireless Communication*, vol. 2007, Article ID: 39871, 2007.

[30] Marvin K. Simon, M. S. Aluoini, *Digital Communication over Fading Channels*, John Wiley and sons publication, second edition, 2005.

[31] I. S. Gradshteyn and I. M. Ryzhik, *Tables of Integrals, Series and Products*, Revised 4th edition, San Diego, CA: Academic, 1980.

[32] K. E. Baddour and N. C. Beaulieu, "Autoregressive Modeling for Fading Channel Simulations", *IEEE Transactions on Wireless Comm.*, vol. 4, no. 4, July 2005.